ME40064 System Modelling and Simulation - Coursework 3

1968 Words, Candidate No. 11973, 9th January 2026
Department of Mechanical Engineering, University of Bath

1. Introduction

Simulating dynamic systems can provide valuable insights into their behaviour under various conditions, but can also introduce challenges such as model accuracy and computation efficiency. For simulating vehicle dynamics, a **half car model** (Figure 1) is often used to isolate the essential characteristics of a car's suspension system while simplifying the complexity of a full car model [1]. It models dynamics along a straight road, providing insight into vertical and pitch motions.

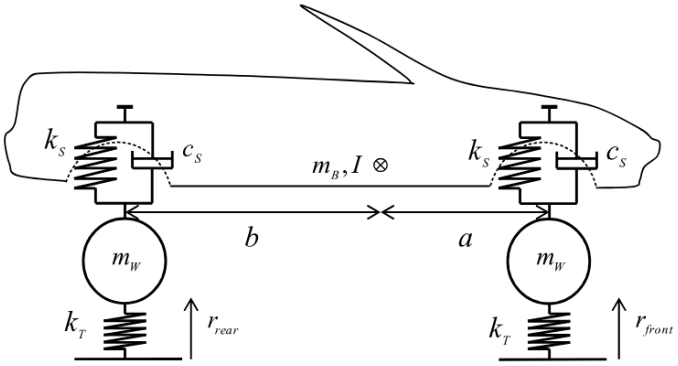

Figure 1: Representation of the Half Car Model [2]

The equations of motion for the half car model are as follows [2]:

$$m_B \ddot{s}_B = F_{\text{front}} + F_{\text{rear}} - m_B g \tag{1}$$

$$I\ddot{\theta} = aF_{\text{front}} - bF_{\text{rear}} \tag{2}$$

Where s_B is the vertical displacement, θ is the pitch angle, m_B is the body mass, I is the moment of inertia, g is gravitational acceleration, and a and b are distances from the center of mass to the front and rear axles respectively. F_{front} and F_{rear} are the forces exerted by the front and rear suspension models, described as a sprung mass in series with a damper and spring.

Simulink is a simulation environment and graphical modelling system, available as part of the MATLAB software suite [3]. It is particularly well-suited for modelling dynamic systems, providing a wide range of solvers and fundamental 'blocks' for constructing models (e.g. Figure 2).

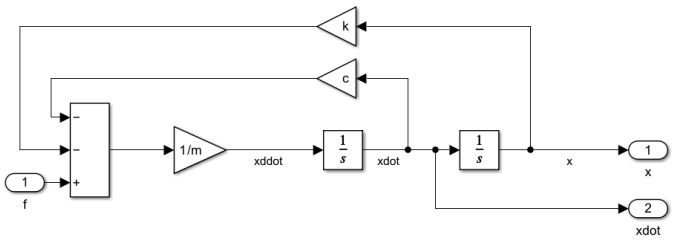

Figure 2: Simulink Spring-Mass-Damper System

2. Part 1: Model Construction and Verification

2.1. Creation of a Half Car Body Block

A Simulink block was created to solve the half car equations of motion. This had inputs of the front and rear suspension forces, and outputs of the body vertical displacement and pitch angle, as well as front and rear axle vertical displacements and velocities (Figure 3, Figure 4).

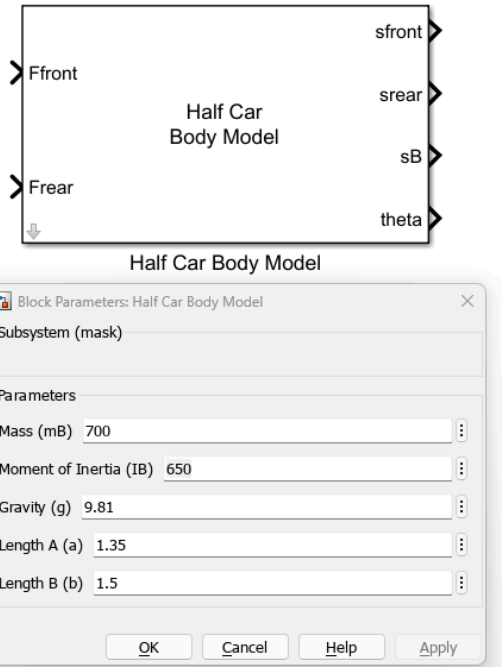

Figure 3: Simulink Half Car Body Block

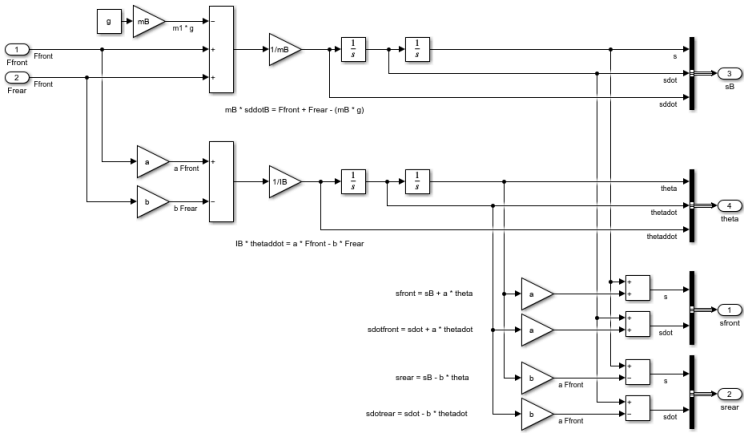

Figure 4: Simulink Half Car Body Block Subsystem

The front and rear vertical displacements and velocities were calculated according to the following equations:

$$s_{\text{front}} = s_B + a\theta, \quad \dot{s}_{\text{front}} = \dot{s}_B + a\dot{\theta} \tag{3}$$

$$s_{\text{rear}} = s_B - b\theta, \quad \dot{s}_{\text{rear}} = \dot{s}_B - b\dot{\theta} \tag{4}$$

2.2. Verification of the Half Car Body Block

A significant benefit of Simulink is the clear definition of inputs and outputs for each block, allowing for modular testing and verification of individual components. For the half-car block, the only inputs were the front and rear suspension forces, alongside the set of parameters defined in the block mask.

The first set of tests focused on Equation 1, analysing the vertical displacement output, while the second set of tests focused on Equation 2, studying the pitch angle output.

2.2.1. Vertical Displacement Tests

First, the effect of the sum of the front and rear suspension forces on the vertical displacement output was investigated.

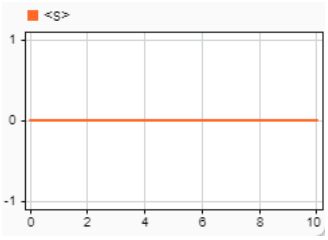

Figure 5: F_{front} and F_{rear} Sum to $m_B g$

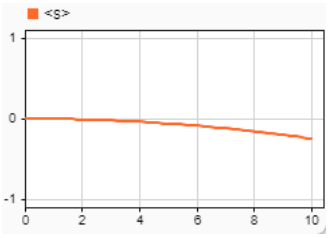

Figure 6: F_{front} and F_{rear} Sum to Less than $m_B g$

In Figure 5, the front and rear suspension forces sum to equal the weight of the car body ($m_B g$), resulting in a balanced system with no change in vertical displacement, as expected from Equation 1. When the suspension force is reduced so that the resultant force is less than the weight of the car body, Figure 6 shows that the car body drops downwards, again as expected.

Next, the effect of the magnitude of the mass m_B on the vertical displacement output was investigated, with a constant resultant force greater than the weight of the car body.

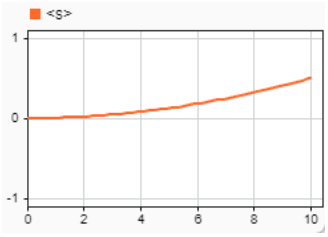

Figure 7: 1N Resultant Upward Force with 100kg Mass

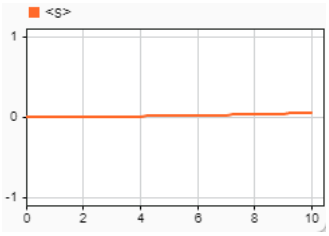

Figure 8: 1N Resultant Upward Force with 1000kg Mass

Figure 7 and Figure 8 show that a lower mass results in a greater vertical displacement response to the same applied force, as expected from Equation 1.

The distance the car body moves in response to the resultant 1N force matches the theoretical values calculated using Newton's second law ($F = ma$) over a 10 second interval.

In addition to this, the suspension force being greater than the weight of the car body results in an upward acceleration, validating the model further.

2.2.2. Pitch Angle Tests

First, the effect of a and b on the pitch angle output was investigated. The ratio of these parameters determines the position of the car's centre of gravity (CG), which should affect the pitch angle response to equal front and rear forces.

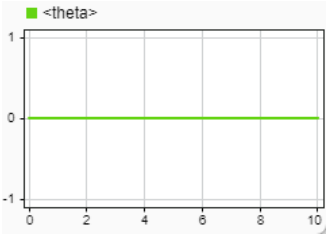

Figure 9: Pitch Angle With Equal Front and Rear Forces, a and b Equal

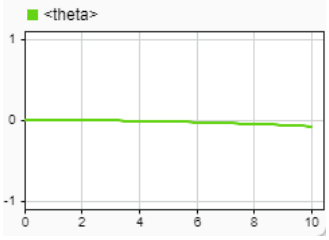

Figure 10: Pitch Angle With Equal Front and Rear Forces, CG Shifted Forward

Figure 9 shows that the pitch angle remains at zero when equal front and rear forces are applied with a and b equal, as expected. When the CG is shifted forwards, while keeping the front and rear suspension forces equal, Figure 10 shows that the car pitches downwards as expected from Equation 2.

Next, the effect of unequal front and rear forces on the pitch angle output was investigated, with a and b kept equal.

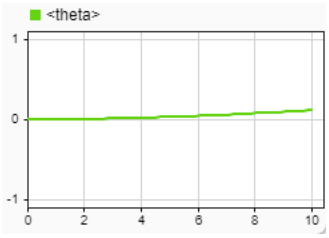

Figure 11: Pitch Angle with Higher Front Force, a and b Equal

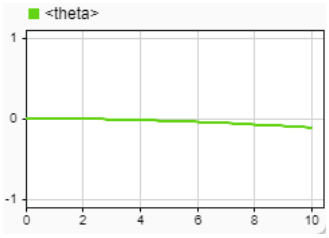

Figure 12: Pitch Angle with Higher Rear Force, a and b Equal

Figure 11 shows that when the front suspension force is higher than the rear, the car pitches upwards as expected from Equation 2. Conversely, Figure 12 shows that when the rear suspension force is higher than the front, the car pitches downwards, again as expected.

Finally, the effect of the moment of inertia I on the pitch angle output was investigated, with a and b kept equal and a higher front suspension force applied.

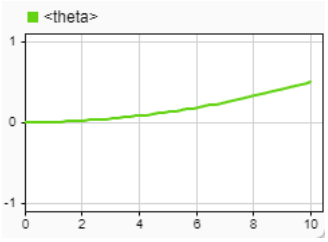

Figure 13: Pitch Angle with Higher Front Force, Lower Moment of Inertia

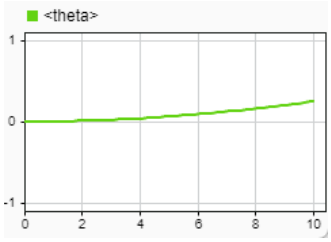

Figure 14: Pitch Angle with Higher Front Force, Higher Moment of Inertia

Figure 13 and Figure 14 show that a lower moment of inertia results in a higher pitch angle response to the same applied forces, as expected from Equation 2.

Test	Result
Body doesn't move with upward force of mg	PASS
Body moves down with upward force < mg	PASS
Lower mass results in greater displacement	PASS
Balanced forces with CG at midpoint results in zero pitch	PASS
CG forward results in nose-down pitch	PASS
Higher front force results in nose-up pitch	PASS
Higher rear force results in nose-down pitch	PASS
Higher moment of inertia results in smaller pitch angle	PASS

Table 1: Half Car Body Block Test Results

2.3. Creation of Full Half Car Model Block

Having validated the half car body block, a full half car model was assembled by coupling it with front and rear suspension and tyre blocks, as shown in Figure 15.

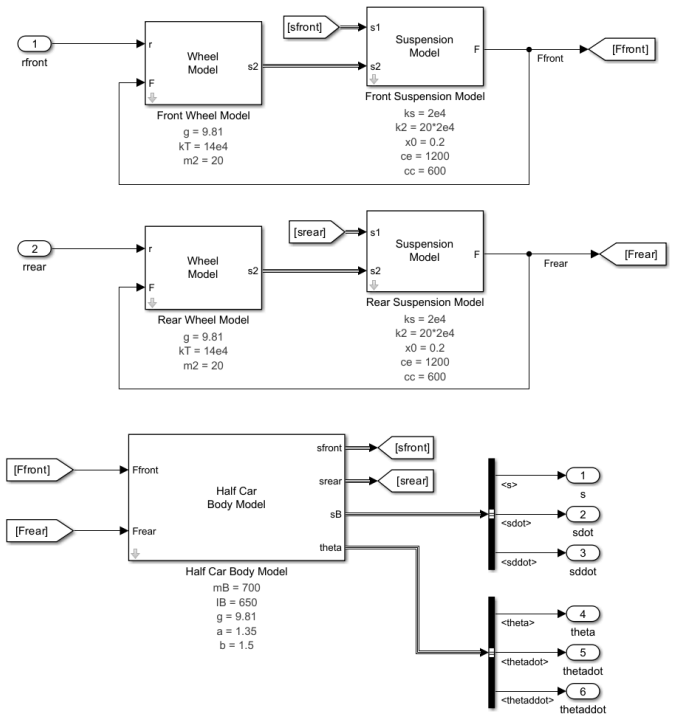

Figure 15: Simulink Half Car Model

The parameters of the suspension, tyre and body models were all set according to the coursework specification [2].

Simulink Goto/From blocks and bus signals were used to manage signal routing and maintain model clarity.

2.4. Verification of the Full Half Car Model

As with the half car body block, a suite of tests was performed to verify the full half car model.

First, the settle response of the car and the effect of mass on settle displacement were investigated.

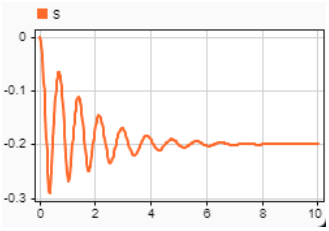

Figure 16: Settle Response with Coursework Mass

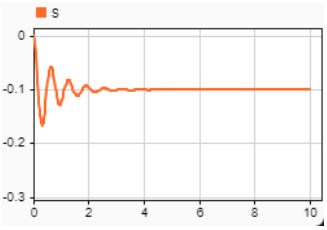

Figure 17: Settle Response with Half Mass

Figure 16 and Figure 17 show that the resultant vertical displacement of the car after settling is correctly affected by the mass of the car body.

Next, the effect of suspension damping on the settle response was investigated.

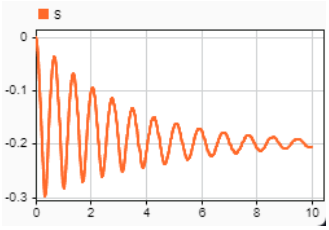

Figure 18: Settle Response with Decreased Damping

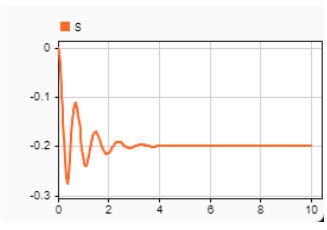

Figure 19: Settle Response with Increased Damping

Figure 18 and Figure 19 show that the damping coefficient of the suspension affects the rate of settling, as expected.

After this, the effect of the CG position on the pitch angle during settling was investigated.

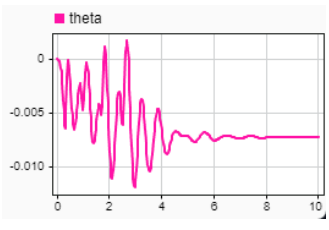

Figure 20: Settle Pitch with Coursework CG Position

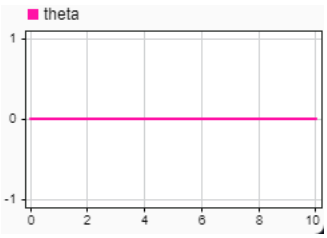

Figure 21: Settle Pitch with CG at Midpoint

Figure 20 and Figure 21 show that under the coursework parameters, the car settles with a small pitch angle due to the CG being forward of centre, with identical front and rear suspension characteristics. When the CG is moved

to the midpoint between the front and rear axles, the car settles with zero pitch angle, as expected.

Next, the response of the car to road steps was investigated, first with a step hitting both front and rear axles simultaneously, and then with a staggered step hitting the front axle before the rear.

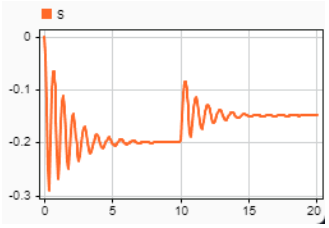

Figure 22: Displacement Response to Step

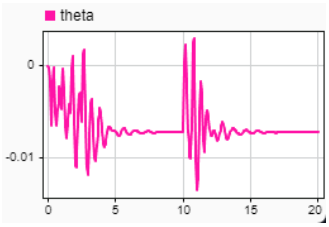

Figure 23: Pitch Response to Step

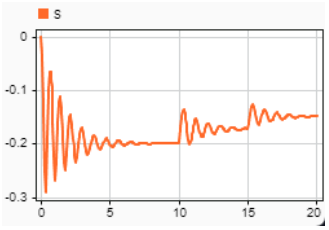

Figure 24: Displacement Response to Staggered Step

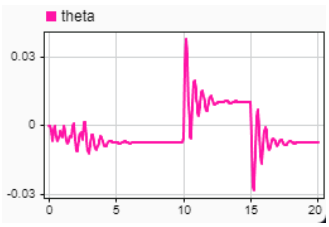

Figure 25: Pitch Response to Staggered Step

These results show that the car responds appropriately to road disturbances.

Test	Result
Settle displacement affected by mass	PASS
Lower damping results in slower settling	PASS
Higher damping results in faster settling	PASS
CG forward results in nose-down pitch during settling	PASS
CG at midpoint results in zero pitch during settling	PASS
Step input results in appropriate vertical and pitch response	PASS
Staggered step input results in appropriate vertical and pitch response	PASS

Table 2: Half Car Model Test Results

2.5. Simulation Convergence

All simulations were run using Simulink's variable step solver [4], with an automatic solver implementation and parameters. These are automatically adjusted to maintain accuracy while optimising computation time. The consistency and physical plausibility of the results across all tests indicate that the simulations converged successfully.

3. Part 2: Investigation of Car Performance

3.1. Sinusoidal Road Profile

A sinusoidal road profile was created to investigate the performance of the half car model under different conditions. The road profile had an amplitude of 0.01m and a wavelength of 1m, and was tested with a range of speeds.

A baseline dataset was captured, for the core performance metrics of body vertical acceleration ($\ddot{s}_B$), body pitch angular acceleration ($\ddot{\theta}$), and front wheel vertical displacement relative to the road ($s_{w,\,\text{front}}$), at speeds of 1m/s and 5m/s.

3.1.1. Baseline Performance

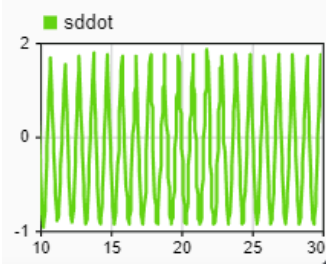

Figure 26: $\ddot{s}_B$ at 1m/s, Nominal Parameters

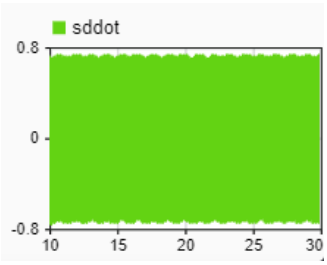

Figure 27: $\ddot{s}_B$ at 5m/s, Nominal Parameters

Figure 28: $\ddot{\theta}_B$ at 1m/s, Nominal Parameters

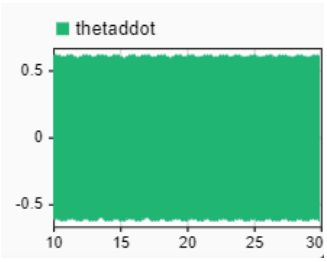

Figure 29: $\ddot{\theta}_B$ at 5m/s, Nominal Parameters

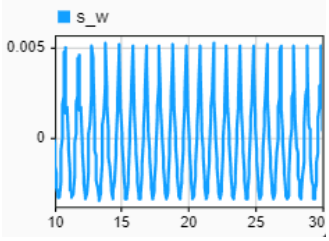

Figure 30: $s_{w,\,\text{front}}$ at 1m/s, Nominal Parameters

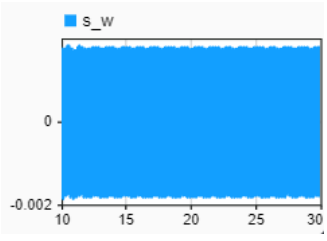

Figure 31: $s_{w,\,\text{front}}$ at 5m/s, Nominal Parameters

3.1.2. Performance with Increased Suspension Stiffness

After establishing the baseline performance, the suspension stiffness was doubled to investigate its effect on the performance metrics.

As specified by the coursework description [2], the spring contants of both front and rear suspensions used a lookup table, so all values in the table were multiplied by 2 to achieve the increased stiffness.

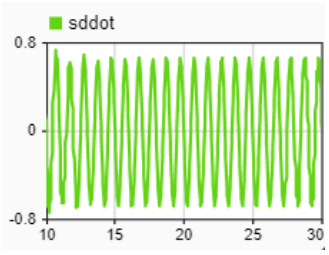

Figure 32: $\ddot{s}_B$ at 1m/s, $2k_s$

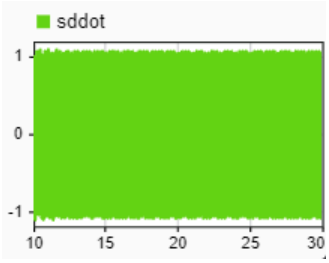

Figure 33: $\ddot{s}_B$ at 5m/s, $2k_s$

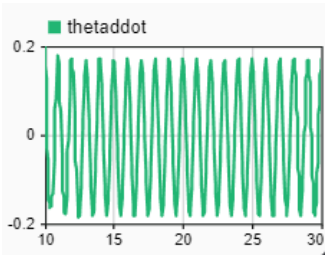

Figure 34: $\ddot{\theta}_B$ at 1m/s, $2k_s$

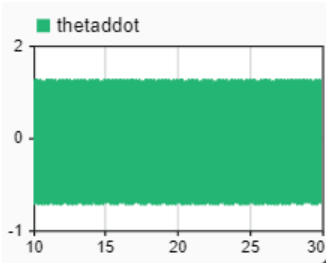

Figure 35: $\ddot{\theta}_B$ at 5m/s, $2k_s$

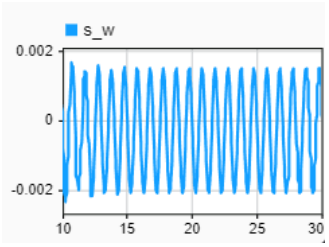

Figure 36: $s_{w,\text{ front}}$ at 1m/s, $2k_s$

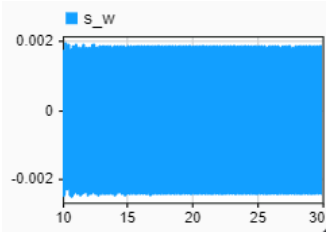

Figure 37: $s_{w,\text{ front}}$ at 5m/s, $2k_s$

The stiffer suspension resulted in a smoother ride at lower speeds, with reduced body accelerations (as shown in Figure 26 vs Figure 32, and Figure 28 vs Figure 34), alongside lower wheel displacement relative to the road (Figure 30 vs Figure 36).

At higher speeds, however, the stiffer suspension led to increased body accelerations (Figure 27 vs Figure 33, and Figure 29 vs Figure 35), indicating a harsher ride. The wheel displacement relative to the road also increased (Figure 31 vs Figure 37), suggesting reduced handling characteristics.

The improved performance at lower speeds can be attributed to the stiffer suspension's ability to better resist body movement in response to changes in road profile, while the degraded performance at higher speeds likely results from a shift in the suspension's natural frequency, leading to an increased amplitude compared to the baseline.

3.1.3. Performance with Increased Suspension Damping

Next, the suspension damping was doubled to investigate its effect on the performance metrics. Also specified by the coursework description [2], the damping coefficients were different depending on if the suspension was in compression or extension.

Both the compression and extension damping coefficients of the front and rear suspensions were therefore multiplied by 2 to achieve the increased damping for analysis.

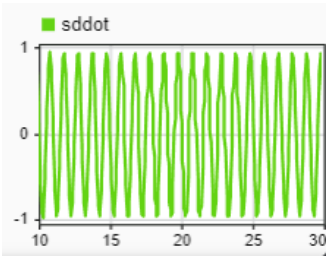

Figure 38: $\ddot{s}_B$ at 1m/s, $2c_s$

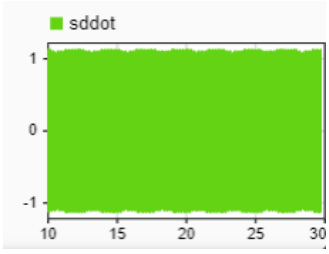

Figure 39: $\ddot{s}_B$ at 5m/s, $2c_s$

Figure 40: $\ddot{\theta}_B$ at 1m/s, $2c_s$

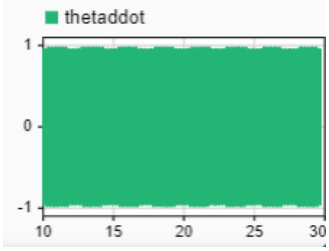

Figure 41: $\ddot{\theta}_B$ at 5m/s, $2c_s$

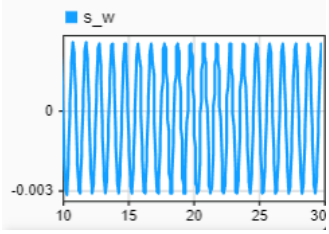

Figure 42: $s_{w,\text{ front}}$ at 1m/s, $2c_s$

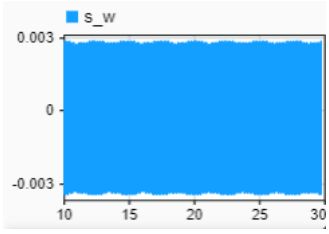

Figure 43: $s_{w,\text{ front}}$ at 5m/s, $2c_s$

As with the increased stiffness case, the increased damping resulted in a smoother ride at lower speeds, with reduced body accelerations (as shown in Figure 26 vs Figure 38, and Figure 28 vs Figure 40), alongside lower wheel displacement relative to the road (Figure 30 vs Figure 42).

Also like the increased stiffness case, at higher speeds the increased damping led to increased body accelerations (Figure 27 vs Figure 39, and Figure 29 vs Figure 41), indicating a harsher ride. The wheel displacement relative to the road also increased (Figure 31 vs Figure 43), and by more than in the increased stiffness case, suggesting further reduced handling characteristics.

At lower speeds, the improved performance is likely due to the increased energy dissipation provided by the higher damping, reducing oscillations in response to road profile changes. At high speeds, however, the dampers may be over-damping the system, making it act more like a rigid body and transmitting more road disturbances to the sprung mass.

3.2. Speedbump Response

3.2.1. Nominal Speedbump Response

A speedbump profile was created in Simulink, based on the Watt profile [5], but with configurable width and height parameters. The initial case had a width of 0.5m and a height of 0.05m.

The response of the core performance metrics of the half car model was then captured at speeds of 5m/s and 10m/s.

Figure 44: $\ddot{s}_B$ at 5m/s, Nominal Speedbump

Figure 45: $\ddot{s}_B$ at 10m/s, Nominal Speedbump

Figure 46: $\ddot{\theta}_B$ at 5m/s, Nominal Speedbump

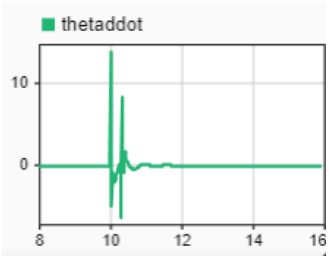

Figure 47: $\ddot{\theta}_B$ at 10m/s, Nominal Speedbump

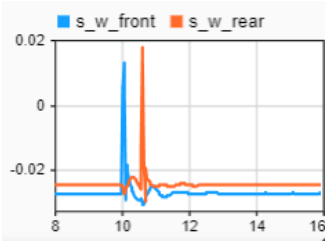

Figure 48: s_w at 5m/s, Nominal Speedbump

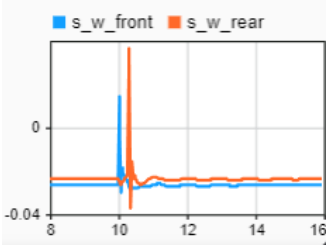

Figure 49: s_w at 10m/s, Nominal Speedbump

3.2.2. Wider Speedbump Response

After capturing the baseline results, the width of the speedbump was increased to 1.0m while keeping the height at 0.05m, and the response was captured again at speeds of 5 and 10m/s.

Figure 50: $\ddot{s}_B$ at 5m/s, Wider Speedbump

Figure 51: $\ddot{s}_B$ at 10m/s, Wider Speedbump

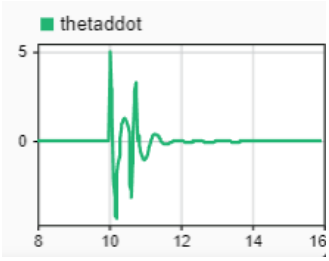

Figure 52: $\ddot{\theta}_B$ at 5m/s, Wider Speedbump

Figure 53: $\ddot{\theta}_B$ at 10m/s, Wider Speedbump

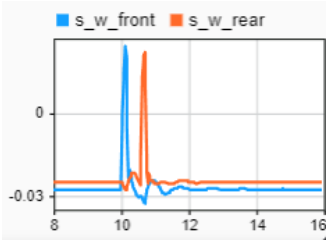

Figure 54: s_w at 5m/s, Wider Speedbump

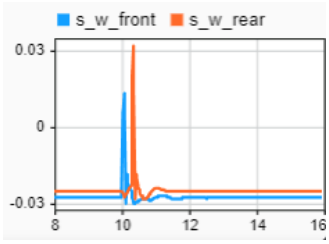

Figure 55: s_w at 10m/s, Wider Speedbump

Comparing these results to the nominal speedbump case, the wider speedbump resulted in a reduced effect on the body accelerations and wheel displacement at both speeds, indicating a less disruptive ride. This is likely due to the more gradual change in road profile provided by the wider bump.

3.2.3. Taller Speedbump Response

Finally, the height of the speedbump was increased to 0.1m while keeping the original width at 0.5m, and the response of the core performance metrics was captured again at speeds of 5m/s and 10m/s.

Figure 56: $\ddot{s}_B$ at 5m/s, Taller Speedbump

Figure 57: $\ddot{s}_B$ at 10m/s, Taller Speedbump

Figure 58: $\ddot{\theta}_B$ at 5m/s, Taller Speedbump

Figure 59: $\ddot{\theta}_B$ at 10m/s, Taller Speedbump

Figure 60: s_w at 5m/s, Taller Speedbump

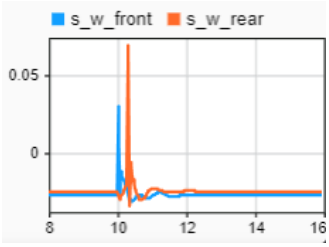

Figure 61: s_w at 10m/s, Taller Speedbump

The taller speedbump resulted in significantly increased body accelerations and wheel displacement at both speeds compared to the nominal case, indicating a much more disruptive ride. This is due to the larger vertical change in road profile, which the suspension must work harder to absorb.

4. Conclusion

Talk about adaptive dampers?

This coursework investigation succesfully developed and validated a half car model in Simulink, demonstrating an accurate representation of vertical and pitch dynamics in a purely longitudal context.

Effective unit testing was performed to validate components of the model, alonside system-level testing to ensure the full model behaved as expected under various conditions.

The sinusoidal road profile analysis highlighted the trade-offs involved in suspension tuning, with increased stiffness and damping improving ride quality at lower speeds but degrading it at higher speeds.

Analysing the response of the model to different speedbump profiles showed a clear relationship between bump geometry and ride comfort, with wider bumps being less disruptive and taller bumps causing significant increases in body accelerations and wheel displacement. There was also a clear trend of increasing severity of response with increasing speed, exactly as a speedbump should behave.

These findings illustrate the limitations of a traditional passive suspension system in handling a wide range of road conditions and speeds. It is therefore understandable that modern vehicles are increasingly adopting adaptive suspension systems, which can dynamically adjust damping and stiffness characteristics in real-time based on road conditions and driving dynamics. Such systems have the potential to significantly enhance ride comfort and handling characteristics across a broader range of scenarios compared to traditional solutions [6].

5. References

[1] H. D. W. Gau N. Zhang, "A Half-car Model for Dynamic Analysis of Vehicles with Random Parameters," 2007. [Online]. Available: https://search.informit.org/doi/epdf/10.3316/informit.221968307621967

[2] A. Cookson, "Assignment 2: Simulink Modelling of Dynamic Systems," 2025.

[3] "Simulink." [Online]. Available: https://mathworks.com/products/simulink.html

[4] "Choose a Solver." [Online]. Available: https://www.mathworks.com/help/simulink/ug/choose-a-solver.html

[5] W Satiennam et al., "Effects of Speed Bumps and Humps on Motorcycle Speed Profiles," 2014. [Online]. Available: https://www.scientific.net/AMR.931-932.536

[6] M. C. U. Demircioglu, "A comparison study of passive, active, and semi-active suspension systems," 2024. [Online]. Available: https://doi.org/10.1504/IJVNV.2024.142742